Available online at www.sciencedirect.com
SCIENCE DIRECT®
Agricultural and Forest Meteorology 125 (2004) 259–277
AGRICULTURAL AND FOREST METEOROLOGY
www.elsevier.com/locate/agrformet

PM_{10} emission from agricultural soils on the Columbia Plateau: comparison of dynamic and time-integrated field-scale measurements and entrainment mechanisms

J. Kjelgaard [a,*], B. Sharratt [b], I. Sundram [c], B. Lamb [c], C. Claiborn [c], K. Saxton [b], D. Chandler [d]

[a] *Environmental Physics Group, Soil and Crop Sciences, Texas A&M University, College Station, TX, USA*
[b] *Land Management and Water Conservation Group, USDA-ARS, Pullman, WA 99164, USA*
[c] *Laboratory for Atmospheric Research, Department of Civil and Environmental Engineering, Washington State University, Pullman, WA 99164, USA*
[d] *Department of Plants, Soils and Biometeorology, Utah State University, Logan, UT, USA*

Received 15 October 2003; received in revised form 7 April 2004; accepted 16 April 2004

Abstract

Emission of particles less than 10 μm mean diameter (PM_{10}) from agricultural sources is an environmental issue due to health concerns and potential effects on local and global climate. The Columbia Plateau region of Washington and Oregon contains vast deposits of fine loess soils and is an active PM_{10} emission source. An instrumented field site was established to continuously monitor meteorological conditions and PM_{10} concentrations at 10 min intervals during periods of high winds (defined as sustained wind speeds >5 m s^{-1} at 2 m height) during the 2001 and 2002 field seasons. Time-integrated measurements of PM_{10} and total soil movement were made using high volume air samplers (HiVols) and BSNE sediment traps, respectively. Particle impact sensors (Sensits®) monitored particle movement (i.e. saltation) close to the surface. Tapered element oscillating microbalances (TEOMs) and wind velocity profiles were utilized to examine short-time-interval dust emission dynamics of fallow, dryland fields. TEOM data clearly identified periods of active PM_{10} emission. TEOM and HiVol PM_{10} concentrations integrated during high wind events (HWE) showed excellent agreement. Time-integrated PM_{10} concentrations were well-correlated with horizontal soil mass transport. However, few saltator impacts were recorded during high wind events. Analysis of wind velocity profiles and friction velocities indicated little saltation was occurring. In general, for continuous emission of PM_{10} from fallow fields with dust mulch conditions, threshold friction velocity was approximately 0.4 m s^{-1} and threshold velocity was approximately 8 m s^{-1}. Several wind events showed evidence where PM_{10} concentration gradients were extremely small, the PM_{10} being well-mixed between 1 and 3 m heights.

Keywords: Wind erosion; Particulates; Friction velocity; Saltation

1. Introduction

Agricultural lands in semi-arid and marginally arid regions represent potential sources of dust (airborne solid particles <60–100 μm mean diameter) during

* Corresponding author. Tel.: +1-979-845-7150; fax: +1-979-845-0456.
E-mail address: jkjelgaard@ag.tamu.edu (J. Kjelgaard).

0168-1923/$ – see front matter © 2004 Elsevier B.V. All rights reserved.
doi:10.1016/j.agrformet.2004.04.004

high wind or high disturbance activities (e.g. tillage operations). A majority of atmospheric dust >2 μm mean diameter is thought to arise from such activity (Pye, 1987). Recent modeling efforts suggest that anthropogenic sources, which include lands used for agricultural production and livestock operations, account for the majority of dust loading on a global basis (Tegen and Fung, 1995; Sokolik and Toon, 1996; Ginoux et al., 2001). Wind blown dust has been recognized as a serious health and environmental issue associated with reduced air quality and visibility (Chepil and Woodruff, 1957; Hagen and Skidmore, 1976; Gillette, 1986), soil nutrient loss (Hagen and Lyles, 1985; Zobeck and Fryear, 1986; Larney et al., 1998), and nutrient/chemical loading on regional ecological systems (Leys, 1999; Leys and McTainsh, 1999).

Recent studies have attempted to characterize dust emissions into the atmosphere (e.g. Brazel, 1989; Butler et al., 2001; Xuan and Sokolik, 2002) and others have specifically examined the contribution of agricultural lands to regional dust concentrations (e.g. Gillette, 1977; Stetler and Saxton, 1996; Shao et al., 1996; Claiborn et al., 1998; Stout, 2001; Goosens and Gross, 2002; Stout and Lee, 2003). Studies examining dust emissions from agricultural lands have primarily emphasized the connection between horizontal soil movement in generating dust emissions and subsequent vertical flux. This has been attributed to saltation or sandblasting (Chepil and Woodruff, 1963; Gillette and Walker, 1977), where sand-sized particles, 70–1000 μm in diameter, bounce along the surface. Such an approach has been incorporated into recent efforts to model dust emissions (e.g. Marticorena and Bergametti, 1995; Shao et al., 1996; Lu and Shao, 1999; Saxton et al., 2000).

An important parameter for estimating/verifying vertical fluxes of suspended particulates (F_A) from a surface is the accurate measurement of particulate concentrations at discreet height intervals (e.g. Gillette et al., 1972; Gillette, 1977; Nickling and Gillies, 1993; Gillette et al., 1997; Saxton et al., 2000). These concentration measurements, which can be used to determine threshold velocity conditions and scale the relative magnitudes of various events, can also be used to estimate F_A with an equation of the form:

$$F_A = \frac{k u_* (C_1 - C_2)}{\ln[z_2/z_1]} \quad (1)$$

where k is von Karman's constant (0.4), u_* the friction velocity (m s^{-1}), and C_1 and C_2 are concentrations (μg m^{-3}) measured at heights (m) z_1 and z_2, respectively. For z_1 lower than z_2, positive fluxes are upward. This version of Eq. (1) assumes neutral or near-neutral atmospheric conditions and that particle settling velocity (υ_p) is negligible. Near neutral atmospheric conditions have been observed during several previous dust events of varying magnitude (Kjelgaard et al., 2004). For suspended particulate matter (PM), if the ratio of $\upsilon_p/u_* < 0.1$, the particles move in a near-gaseous manner (Gillette et al., 1974). Threshold u_* of particles smaller than 10 μm in diameter are typically greater than about 0.2 m s^{-1} for agricultural soils in Texas (Gillette, 1977) and approximately 0.4 m s^{-1} for agricultural soils on the Columbia Plateau (Kjelgaard et al., 2004). Following Shao (2000), a υ_p for 10 μm particles was estimated (∼0.008 m s^{-1}) with the resulting υ_p/u_* ratio being $\ll 0.1$.

Several methods have been employed to measure concentration gradients including time-integrated measurements by high-volume (HiVol) air samplers, low-volume (LoVol) air samplers, and passive samplers (e.g. Cahill et al., 1996; Goosens et al., 2001; Goosens and Gross, 2002; Gomes et al., 2003). Instrumented towers with near-isokinetic total suspended particulate (TSP) samplers have also been utilized (e.g. Gillette et al., 1974; Nickling, 1983; Nickling and Gillies, 1993; Nickling et al., 1999). Others have relied upon stationary and portable wind tunnels to generate soil erosion and dust fluxes (e.g. Bagnold, 1941; Zingg, 1951; Gillette et al., 1974; Fryear, 1984; Raupach and Leys, 1990; Shao et al., 1993; Saxton et al., 2000).

While these methods have provided valuable insights into particulate matter concentration and flux dynamics, they also have limitations. Discrete field sampling via HiVols or LoVols can be limited by the amount of time required to exchange samplers, the total number of samplers available, sample loss during handling, or adverse conditions preventing sampling (Gillette et al., 1997; Lopez, 1998; Ono et al., 2000). Wind tunnel experiments allow for well-controlled and repeatable measurement conditions, but usually involve very short time intervals (e.g. 1–10 min runs) compared to natural wind events, which may last for several hours. Wind tunnels may also require the

introduction of abraders (e.g. Pietersma et al., 1996; Horning et al., 1998; Houser and Nickling, 2001) in order to sustain dust emissions. Wind tunnel size and length may limit the development of the surface boundary layer and therefore not accurately simulate field conditions (Anderson and Haff, 1991; Raupach, 1991; Shao, 2000).

For several years a multidisciplinary research project has examined wind erosion and dust emissions in the Columbia Plateau region of the US Pacific Northwest (PNW) (Saxton, 1995; Stetler and Saxton, 1996; Horning et al., 1998; Saxton et al., 2000). An emphasis of the project has been on the emissions of fine particulate matter smaller than 10 μm mean diameter (PM_{10}) from the extremely fine loess deposits that characterize regional soils (Marks, 1996). Only event-integrated measurements of PM_{10} emissions, along with wind tunnel studies that introduced abrader particles to sustain dust production, have been available from prior years of research. These soils are seasonally subjected to high wind events (HWE) and, in combination with agricultural related activities and climate, are primary contributors to regionally elevated PM_{10} concentrations (Claiborn et al., 1998), a concern due to possible health effects (Glenn and Craft, 1986; Donaldson and MacNee, 1998; Pope and Dockery, 1999). The soils display little evidence of surface scouring or large-scale deposition occurring after high wind events and analyses of horizontal soil transport and vertical dust flux did not follow expected trends based on conventional soil transport models (Stetler and Saxton, 1996).

Recently, Kjelgaard et al. (2004) examined the entrainment processes for two large regional Columbia Plateau dust storms using the wind profile analysis procedures of Gillette (1999) and Raupach (1991). They found little modification of the wind profile or surface roughness length due to saltation loads despite the fact that event-averaged PM_{10} concentrations were relatively high, 1500 and 2800 $\mu g\,m^{-3}$ at 1.5 m, respectively. Examination of particle mass and size distributions with height from event-averaged sampler measurements showed no shift of modal particle range with height from 0.1 to 1.5 m, in contrast to similar studies (Leys and McTainsh, 1996). Limited continuous PM_{10} emission data from a smaller dust event in 2001 showed minimal elevated PM_{10} concentrations prior to the expected PM_{10} ejection threshold friction velocity as estimated with the equation of Marticorena and Bergametti (1995). Had there been a significant amount of larger particles in saltation, finer particles would likely have been dislodged through surface bombardment or particle abrasion and increased PM_{10} levels at lower wind velocities. Therefore, it was recommended that wind erosion and dust emission algorithms account for direct suspension of fine particulates when modeling or measuring soil losses in this region.

Little information is available that documents dust emissions from agricultural fields using continuous sampling devices. Such data can be useful in determining the principle mechanism for entrainment (saltation versus direct suspension) as well as characterizing the dynamics of dust emissions associated with meteorological observations. The primary objectives of this study were to (1) compare10 min interval and time-integrated measurements of PM_{10} from an agricultural field, (2) characterize fluctuations in meteorological factors and PM_{10} emission, and (3) identify and confirm the primary entrainment processes for PM_{10} emissions. A future paper will examine short-time-interval PM_{10} vertical flux during selected high wind events.

2. Analysis

Surface parameters such as friction velocity (u_*) and roughness height (z_0) may be determined by analyzing wind velocity profiles. These parameters are extremely useful in scaling and modeling wind erosion and dust emission events. They may also be utilized to determine the near-surface transport processes, most notably the presence or absence of saltation (Owen, 1964; Raupach, 1991; Gillette, 1999).

The logarithmic wind profile for neutral conditions can be described by

$$u_z = \frac{u_*}{k} \ln\left(\frac{z}{z_0}\right) \quad (2)$$

where u_z is the wind speed at height z and k is von Karman's constant (0.4). Both u_* and z_0 are determined by regression analysis of wind velocity versus the natural log (ln) of the corresponding anemometer heights. The u_* term is the product of the linear regression slope and von Karman's constant k(0.4) and

z_0 is the exponential of the slope intercept divided by the negative of the regression slope.

Atmospheric stability can be assessed by Richardson's number (Ri), which is calculated from wind speed and temperature gradients (Sutton, 1953):

$$Ri = \frac{(g/T)(\gamma_d + (\partial T/\partial z))}{(\partial u/\partial z)^2} \quad (3)$$

where g is the gravitational constant (9.81 m s^{-2}), T the mean temperature (K), ∂_d a constant (−0.0098 K m^{-1}), and ∂T (K) and ∂u (m s^{-1}) are the temperature and wind speed differences over height, ∂z (m). Atmospheric stability conditions were characterized following Thom (1975).

Ideally, determination of u_* and z_0 requires a high degree of linearity (e.g. coefficient of correlation (r^2) ≥ 0.95 or greater) depending on the number of measurement heights comprising the individual wind velocity profile (Stull, 2000). No corrections were made for roughness displacement height, due to bare, fallow conditions; nor for atmospheric stability, due to strong surface winds. Data for analysis were selected based on sustained wind speeds, and screened for wind direction, increasing wind speed with height, debris influencing lower anemometer heights, and general operation.

The coefficient of drag (C_d) for a surface may be defined as

$$C_d = \left(\frac{u_*}{u_z}\right)^2 \quad (4)$$

where u_z is wind speed (m s^{-1}) at a particular reference height z. A constant ratio of u_*/u_z under varying wind velocities indicates that neither C_d nor z_0 are changing. This is demonstrated graphically by plotting u_* versus u_z. A linear relationship of constant slope (Gillette et al., 1997, 1998) indicates little or no saltation. Gillette et al. (1998) found that during saltation, changes in u_* were proportional to $(u_z - u_t)^2$ where u_t is the erosion threshold wind velocity.

Horizontal soil flux was estimated using passive sediment traps, BSNEs (Fryear, 1986). These traps incorporate fine mesh venting and a wedge-like shape to attain near-isokinetic inlet velocities (Shao et al., 1993). The overall efficiency of BSNE samplers for Ritzville soils was 65% as determined by wind tunnel tests with an isokinetic sampling standard. The adjusted BSNE data was plotted against height and fit with a two parameter exponential of the form:

$$q = a\, e^{bz} \quad (5)$$

where q is the mass flux (kg m^{-2}), a and b the fitting parameters and z is height (m). The equation is similar to a four-parameter model utilized previously (Saxton et al., 2000) and consistently produced high correlation coefficients ($r^2 \geq 0.98$). The formula was integrated from 0 to 1.5 m height and a time-integrated mass transport rate per meter width of field per wind event (Q_e: kg m^{-1} per event) was calculated.

Wind energy per event (W_e; MJ event^{-1}) was calculated with the following equation:

$$W_e = \frac{0.5\rho_{air}\sum_0^n u^3\, \Delta t/A}{10^6} \quad (6)$$

where ρ_{air} is air density (1.2 kg m^{-3}), u the wind speed (m s^{-1}) at 2 m height, n the number of measurement intervals where u was greater than or equal to the estimated threshold velocity for PM_{10} (u_{t-10}), Δt the time interval for average velocity (600 s), and A is flow area (m^2). The flow area is a plane normal to the surface and to the mean wind direction, centered about the height of the wind measurement; for our calculations we used a 1 m^2 area. Based on previous analysis, u_{t-10} was estimated to be approximately 8 m s^{-1} for Ritzville soils in loose, dust mulch conditions.

3. Materials and methods

The Columbia Plateau, located in north-central Oregon and south-central Washington, is a region with extensive loess deposits where up to 90% of particles (by mass) can have diameters less than 100 μm (U.S.D.A., 1967). The Plateau is bounded by mountainous terrain on all sides and the Columbia River to the west. Large regions of the Plateau are relatively flat. The depth of loess deposits range from a few centimeters to 45 m (Campbell, 1962). The area is typified by numerous large fields in dryland wheat production that are managed in a crop-fallow rotation (i.e. 1 year the field is planted/harvested and the next year it is left dormant and bare).

The predominant soil type is Ritzville silt loam (Andic Aridic Haplustoll), a mixture of loess, volcanic ash particles, and very low (<1.0%) organic

matter. The fallow fields are subject to a variety of machinery operations such as disking, to incorporate organic residues, and rod-weeding to reduce parasitic water-use by weeds and develop a soil surface moisture barrier. Seeding operations for winter wheat occur in August and September when surface soils are typically dry and strong winds prevail from the west and south. Each of these farming operations progressively breaks down the surface soil structure which results in a dust-mulch that is highly susceptible to wind erosion.

The research field site was established on a 9 ha (300 m × 300 m) subsection in the north-east corner of a large, relatively level 313 ha field. Erosive winds were generally out of the South and West, which allowed a fetch of at least >300 m and as much as 1 km during years when the entire field was fallow (2002). The field was located 11 miles northwest of Washtucna, WA (46°50′N, 118°30′W; 510 m m.s.l.). This site was dedicated to observing temporal changes in soil and dust emissions from bare, disturbed agricultural soils and supplemented an ongoing field campaign of meteorological and time-integrated soil and PM_{10} measurements conducted in commercial agricultural fields (Saxton, 1995). The majority of data presented was collected during Fall 2002 with some additional information from a wind event during Fall 2001.

Particle size distributions (PSD) for the Ritzville silt loam were determined using laser diffraction. Laser diffraction particle size analyses were performed on two sets of soil samples. In 1999, soil samples from several fields, where emission measurements had been taken, were collected, pretreated to remove carbonates and organic matter, and dispersed in a sodium hexametaphosphate solution prior to analysis (i.e. strongly dispersed). In 2001, soil was sampled from the intensive site, run through a 125 μm wire sieve via a Ro-Tap® operated for 2 min. Samples from the finer-than-125 μm fraction were placed in de-ionized water and analyzed (i.e. weakly dispersed). The laser-sizer had particle size ranges of 0.01–800 μm (Mastersizer S, Malvern Instruments, Inc., Southborough, Massachusetts).

Instrumentation at the site consisted of (1) a meteorological/wind velocity profile station, (2) tapered element oscillating microbalance (TEOM) particulate matter monitors, (3) sonic anemometer tower, (4) high-volume air samplers (HiVol), and (5) Big Spring Number Eight (BSNE) sediment traps. The site was supplied with 120 VAC power. Visitation and maintenance of the site was accomplished on a weekly basis throughout the season with additional visits after dust events to ensure the integrity of the instrumentation and collect event data.

The meteorological station (MS) utilized a datalogger (Model 23X, Campbell Scientific Inc., Logan, Utah) to record and control operations. Three-cup anemometers (Model 14A, Met One; Grants Pass, Oregon) and fine-wire (0.13 mm), type T thermocouples (TC) were placed at heights of 0.1, 0.5, 1, 2, 3, and 5 m. Two pairs of TCs were wired differentially (the 0.5–5 and 1–3 m pairs) to allow for more accurate readings of temperature differences. Wind direction (Model 024A, Met One; Grants Pass, Oregon) was monitored at 2 m. A relative humidity (RH)/air temperature probe (Model CS500, Campbell Scientific Inc., Logan, Utah) was placed at 2 m. Additional instrumentation included an aspirated, infrared thermometer (Kjelgaard et al., 1996) to monitor soil surface temperature, a net radiometer (Radiation Energy Balance Systems; Seattle, Washington), a pyranometer (Li-Cor, Inc; Lincoln, Nebraska), a tipping bucket rain gauge (Texas Electronics; Dallas, Texas), soil heat flux plates (Radiation Energy Balance Systems; Seattle, Washington) placed at 10 cm, and type T soil TCs placed at 5 and 15 cm. Radiation sensors, infrared thermometers, and rain gauge were calibrated prior to deployment Soil moisture was determined gravimetrically by taking periodic samples from the upper 10 cm of soil.

Sampling time for the MS instrumentation was 0.1 Hz. Under normal conditions, climate data were averaged over 30-min and 24-h periods. A high wind event was defined as $5\,m\,s^{-1}$ or greater wind velocity at 2 m height maintained for at least 10 min. This standard was based on several years of prior data collection where the criterion was $6.35\,m\,s^{-1}$ (1-min averages) at 3 m height (Stetler and Saxton, 1997). The height was changed to better integrate our site information with an independent regional meteorological station network (Ley and Muzzy, 1992). The lower height and longer integration time for our study warranted a corresponding reduction in threshold velocity for defining a HWE (Stetler and Saxton, 1997). During a HWE, surface temperature, relative

humidity, solar radiation, air temperature profiles and differences, and wind velocity profiles were recorded every 10 min. This rate of data collection ceased when 2 m wind speed remained below 5 m s^{-1} for 15 consecutive minutes.

In an effort to obtain detailed PM_{10} concentration and gradient measurements, tapered element oscillating microbalances (Patashnick and Rupprecht, 1991) were installed at the site. The TEOM is an active sampling technique and an accepted method for measuring PM_{10} concentrations at urban sites (Soutar et al., 1999). PM concentrations were monitored continuously with two TEOM units (Model 1400ab, Rupprecht & Patashnick Co., Inc.; Albany, New York) fitted with PM_{10} cut-off inlets. Inlets were placed at 1 and 3 m heights. A microprocessor recorded concentrations continuously at 10-min intervals.

Sonic anemometers (Models K and Sx, Applied Technology, Inc.; Longmont, Colorado) were mounted on a three-sided, open-grid tower at heights of 1 and 3 m. Instrument booms were facing the south–west. Under normal conditions, u, v, and w wind components and temperature were measured every minute and averaged values were recorded every 30 min using a laptop computer. When a HWE occurred, a signal from the MS triggered continuous collection of sonic anemometer data at 10 Hz. At the same tower, a datalogger (Model 21X, Campbell Scientific Inc., Logan, Utah) collected output from two ground-level Sensit® particle impact sensors (Model H11, Sensit Company; Portland, North Dakota) at 0.1 Hz intervals. The Sensit is a fast-response instrument that utilizes a ring of piezoelectric material surrounding a steel core to convert particle impacts to instrument counts. The sensing element was mounted at ground-level and represents an impact area of approximately 500 mm^2. Data were output at 30-min intervals under normal conditions and at 1-min intervals during HWEs. Both Sensits were tested in a wind tunnel with bulk soil samples from the research site prior to field installation.

Time-integrated concentrations of PM_{10} were monitored with two opposing-jet, constant flow PM10 high-volume air samplers (Model PM 10; Graseby-Anderson, Villlage of Cleves, OH). The samplers are U.S. E.P.A. approved and have approximate lower operating limit of 5 $\mu g\,m^{-3}$ and an upper operating limit in the 400–1000 $\mu g\,m^{-3}$ range (Lodge, 1989). The units were mounted at 3 and 5 m heights and were activated to start when a HWE began. Conversely, the HiVols were deactivated when wind speed was less than 5 m s^{-1} for 15 consecutive minutes. Power for the HiVols was provided by 120 VAC on site. High volume filters were removed at the same time that the BSNE samples were collected; the filters were equilibrated to laboratory conditions for at least 24 h prior to weighing.

Streamwise soil erosion was measured using nine sets of BSNE (Fryear, 1986) airborne soil collectors arranged on a 3 × 3 grid with 20 m spacing between clusters. A cluster consisted of 5 BSNEs mounted to a pole at heights of 0.1, 0.2, 0.5, 1, and 1.5 m. Two creep samplers (USDA/ARS; Big Springs, Texas) were placed at ground-level on the windward side of the instrumentation line. Sample collections were periodic depending on the occurrence and magnitude of HWEs. Samples were air-dried only if the BSNE samplers had collected water during the sampling period. A mean sample mass was calculated for each collection height.

4. Results

4.1. Soil conditions

Soil conditions were mostly dry throughout much of the 2002 season. The entire field (research site and surrounding field) were essentially bare with a layer of dust mulch (5–15 cm thick) in late-August 2002. Approximately 1 mm of rain fell on the research site in mid-August. The surrounding field was planted shortly afterwards and the research site was disked to create a similarly disturbed surface and disrupt any physical soil crust. An additional 2 mm of rain fell on day-of-year (DOY) 276 (10/03/02) and formed a physical soil crust. On DOY 281 (10/08/02) a rod-weeding operation was performed over the 9 ha research site to disrupt this crust, which persisted over the surrounding field. This treatment effectively limited soil emissions to the research site for subsequent wind events. No precipitation after DOY 276 was recorded at the research site until early November, DOY 312.

Field soil PSD analysis results are shown in Fig. 1. The mean particle diameter for these soils was approximately 45 μm and the predominant particle sizes ranged from approximately 30–70 μm. The laser-sized

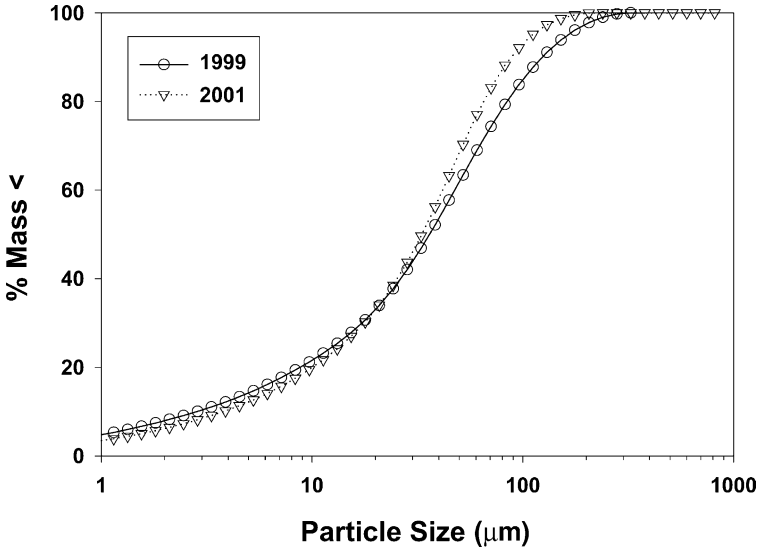

Fig. 1. Particle size distribution for Ritzville silt loam surface soil samples by dispersed laser diffraction.

fractions smaller than 90 μm were approximately 80% and slightly more than 20% of soil particles were PM_{10} or smaller. There was little difference between strongly and weakly dispersed treatments, indicating that smaller particles are not strongly bound to larger ones for these soils. This result is consistent with the low organic matter and overall lack of aggregation observed in rod-weeded fields.

4.2. Time-integrated PM_{10} concentrations and soil erosion

The TEOMs allowed for near-continuous collection of 10-min interval readings of PM_{10} at the site. A week of TEOM, wind speed and wind direction data from DOY 241–247 is shown in Fig. 2. The output clearly displays time periods when PM_{10} levels

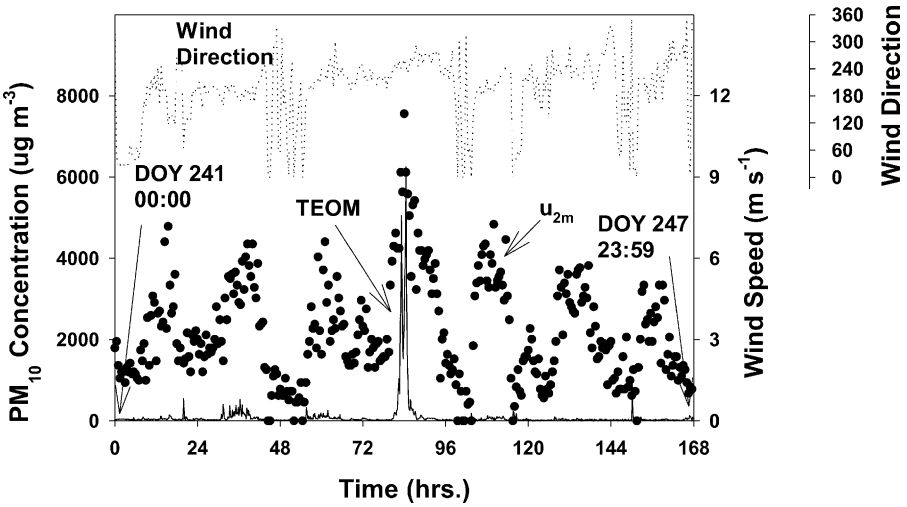

Fig. 2. Continuous 10-min PM_{10} concentration measured by the TEOM at 3 m height (solid line), continuous 30-min wind speed at 2 m height (solid circles), and wind direction (dotted line) for day-of-year (DOY) period of 241–247, 2002 (08/29/02 to 09/04/02).

were elevated. One period of particularly gusty winds (DOY 243, hours 48–72) caused slightly elevated PM_{10} levels but did not qualify as a HWE. However, this was not seen in other weekly periods. Isolated peaks in the TEOM readings were primarily attributed to traffic on a nearby gravel road running north–south and located 50 m directly east of the site; these spikes often occurred when winds/breezes were from the east. Occasional dust devils were also observed traveling through the site.

The time-integrated PM_{10} concentrations measured by the HiVols were calculated based on gravimetric methods, site calibrated inlet flow rates, and elapsed time of operation, usually totaling 5–10 days. Likewise, time-integrated concentrations measured with the TEOMs were determined by summing and averaging all the 10-min PM_{10} readings that corresponded with HWE 10-min data collected by the MS. For example, Fig. 2 contained five HWEs during the DOY 241–247 period; the time-integrated TEOM PM_{10} concentration was the average of all 10-min TEOM measurements taken during the HWEs. A bar graph showing seven weekly periods of time-integrated PM_{10} concentrations for HiVol (3 m height) and $TEOM_{3m}$ is shown in Fig. 3a. In most instances, the results were within ±5%. The cumulative TEOM filter mass for the weekly readings are also shown in Fig. 3a. The TEOM filters were changed periodically following manufacturer recommended intervals. On weeks DOY 275–282, the 3 m HiVol sampler motor malfunctioned and no comparison was made; time-integrated TEOM PM_{10} concentrations for that period were less than 30 $\mu g\,m^{-3}$. Of the seven DOY periods shown in Fig. 3a, five had substantial HWEs that resulted in measurable BSNE catch and PM_{10} emission. A scatter-graph of the TEOM versus available HiVol PM_{10} concentrations compared to a 1:1 line is shown in Fig. 3b and shows good agreement except for one outlier (discussed below).

The BSNE data provided estimates of horizontal soil mass transport. Results comparing Q_e estimated with Eq. (5) versus a four-parameter exponential function used on these soils previously (Saxton et al., 2000) showed excellent agreement. Therefore, the two-parameter Q_e estimates were considered accurate. Event-integrated wind energy (W_e) compared to horizontal soil mass transport (Q_e) and TEOM PM_{10} concentrations are shown in Fig. 4. The linear correlation of W_e and Q_e is evident ($y = 0.248x$, $r^2 = 0.93$). The plot of W_e and PM_{10} concentrations exhibits less linear correlation (Fig. 4b). Time-integrated measurements of PM_{10} concentration from the 5 m HiVol were also included during four periods when data were available (Fig. 4b). The differences in PM_{10} concentrations at 1, 3, and 5 m heights, typical of measurements often used to estimate PM_{10} fluxes, decreased with increasing W_e. The pattern seen in Fig. 4b was also exhibited when PM_{10} concentrations were plotted against soil transport.

4.3. Dynamic PM_{10} concentrations

The primary advantage of the TEOM air sampler is the ability to collect PM concentrations over relatively short-time steps. As noted in Fig. 3a, several HWEs occurred in 2002 that had substantial periods of continuous 10-min interval PM_{10} data collected. An additional HWE from the site in 2001 also had 10-min TEOM data available. This section will present dynamic PM_{10} concentration and meteorological data from four representative HWEs.

Examples of dust storms that produced relatively well-mixed PM_{10} concentrations throughout the 1–3 m heights, both during the 2002 season, are seen in Fig. 5. The event on DOY 244 (Fig. 5a) was a relatively intense storm. Periods of steadily increasing PM_{10} concentrations were from 10:00 to 12:30 though elevated concentrations persisted from 8:30 through 21:30. The average PM_{10} concentrations at 1 and 3 m, averaged over the entire high wind period, were approximately 691 and 672 $ug\,m^{-3}$, respectively. However, the standard deviations were an order of magnitude larger, 1371 and 1255 $ug\,m^{-3}$, respectively, and demonstrates that the range of concentrations measured at 10-min intervals was quite variable. The average wind speed at 2 m height was $8.7 \pm 1.4\,m\,s^{-1}$ and from the southwest. The average u_* and z_0 values, respectively, were $0.54 \pm 0.09\,m\,s^{-1}$ and 0.003 ± 0.002 m. Using Eq. (1), the average PM_{10} flux was 4 $ug\,m^{-2}\,s^{-1}$, with a standard deviation of 15 $ug\,m^{-2}\,s^{-1}$. The maximum and minimum PM_{10} flux rates were 87 and -12 $ug\,m^{-2}\,s^{-1}$, respectively. The HWE on DOY 272 (Fig. 5b) was characterized by average wind speeds of $7.6 \pm 2.6\,m\,s^{-1}$ (2 m height), u_* of $0.47 \pm 0.16\,m\,s^{-1}$, and z_0 values of 0.004 ± 0.002 m. Winds were also from the southwest. The average PM_{10} concentrations

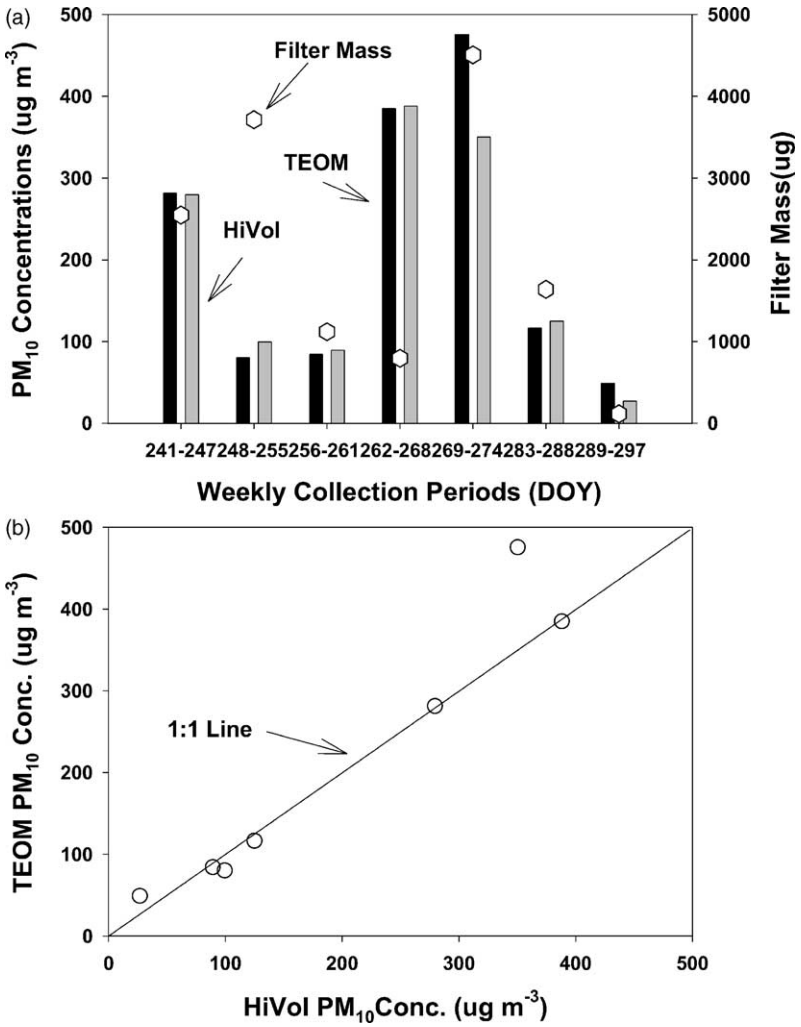

Fig. 3. Time-integrated PM_{10} concentrations ($\mu g\,m^{-3}$) at 3 m height from TEOM and high volume air samplers (HiVol): (a) for several day-of-year (DOY) collection periods and TEOM filter mass at the end of collection periods; (b) comparison of TEOM vs. HiVol data.

were 769 and 802 ug m^{-3} at 1 and 3 m, and a common standard deviation of approximately 1135 ug m^{-3}. The event-averaged concentration was slightly larger at 3 m height and was primarily due to a few isolated periods when the PM_{10} concentrations at 3 m were considerably greater than 1 m concentrations. The average PM_{10} flux was -6 ug $m^{-2}\,s^{-1}$, with a standard deviation of 32 ug $m^{-2}\,s^{-1}$. The maximum and minimum PM_{10} flux rates were 50 and -232 ug $m^{-2}\,s^{-1}$, respectively. The 1-min results of the Sensit® impact sensors showed very few impacts during the course of either storm (Fig. 5) with 4 and 10 total impacts, respectively, for the 244 and 272 events.

Two HWEs (DOY 285 in 2001 and DOY 283 in 2002) were recorded that displayed well-developed PM_{10} gradients between 1 and 3 m heights. The DOY 285 event (Fig. 6a) had an average wind velocity of $7.2 \pm 2.2\,m\,s^{-1}$, and average u_* and z_0 values of $0.44 \pm 0.15\,m\,s^{-1}$ and 0.003 ± 0.002 m, respectively. The TEOM data from 1 m was only available after 11:30, due to an internal memory overload, and data from 14:40 to 15:10 from both TEOMs was discarded

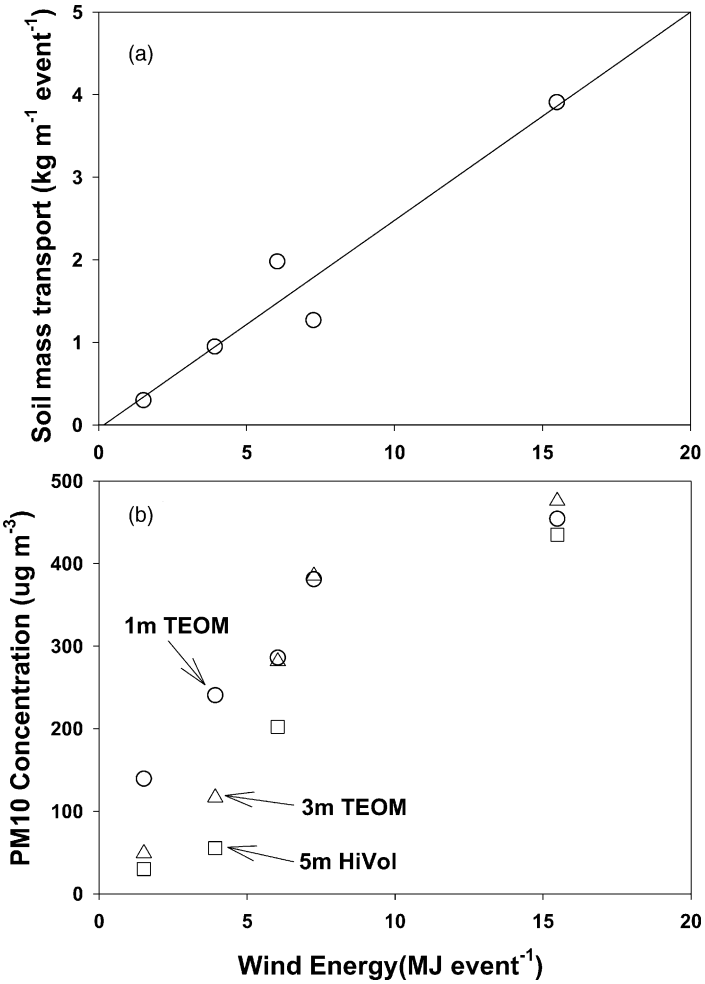

Fig. 4. Relationship between time-integrated measurements of wind energy and (a) horizontal soil mass transport; (b) PM_{10} concentrations for DOY periods with substantial soil mass transport.

due to personnel activity around the sensors during that time. The site at that time had 30% residue ground cover. The average PM_{10} concentrations at 1 and 3 m TEOMs were 291 and 211 ug m^{-3}, respectively, with standard deviations of 254 and 199 ug m^{-3}. Using Eq. (1), the average PM_{10} flux was 16 ug m^{-2} s^{-1}, with a standard deviation of 16 ug m^{-2} s^{-1}. The maximum and minimum PM_{10} flux rates were 55 and -14 ug m^{-2} s^{-1}, respectively. The 283 event (Fig. 6b) had average winds of 7.5 ± 1.4 m s^{-1} and average u_* and z_0 values of 0.43 ± 0.11 m s^{-1} and 0.002 ± 0.002 m, respectively. The average PM_{10} concentrations were 286 and 138 ug m^{-3} at 1 and 3 m, respectively, with standard deviations of 439 and 191 ug m^{-3}. The average PM_{10} flux was 25 ug m^{-2} s^{-1}, with a standard deviation of 47 ug m^{-2} s^{-1}. The maximum and minimum PM_{10} flux rates were 258 and -2 ug m^{-2} s^{-1}, respectively. The Sensits® recorded only four total impacts during the DOY 283 event; no readings were available for the DOY 285 event.

The relationship between PM_{10} emissions and u_* was examined for the events shown in Figs. 5 and 6. Prior analysis of the correlation between TEOM measurements and wind velocity for the DOY 285 event (Fig. 6a) showed slightly better correlation between $TEOM_{1m}$ PM_{10} concentrations and wind

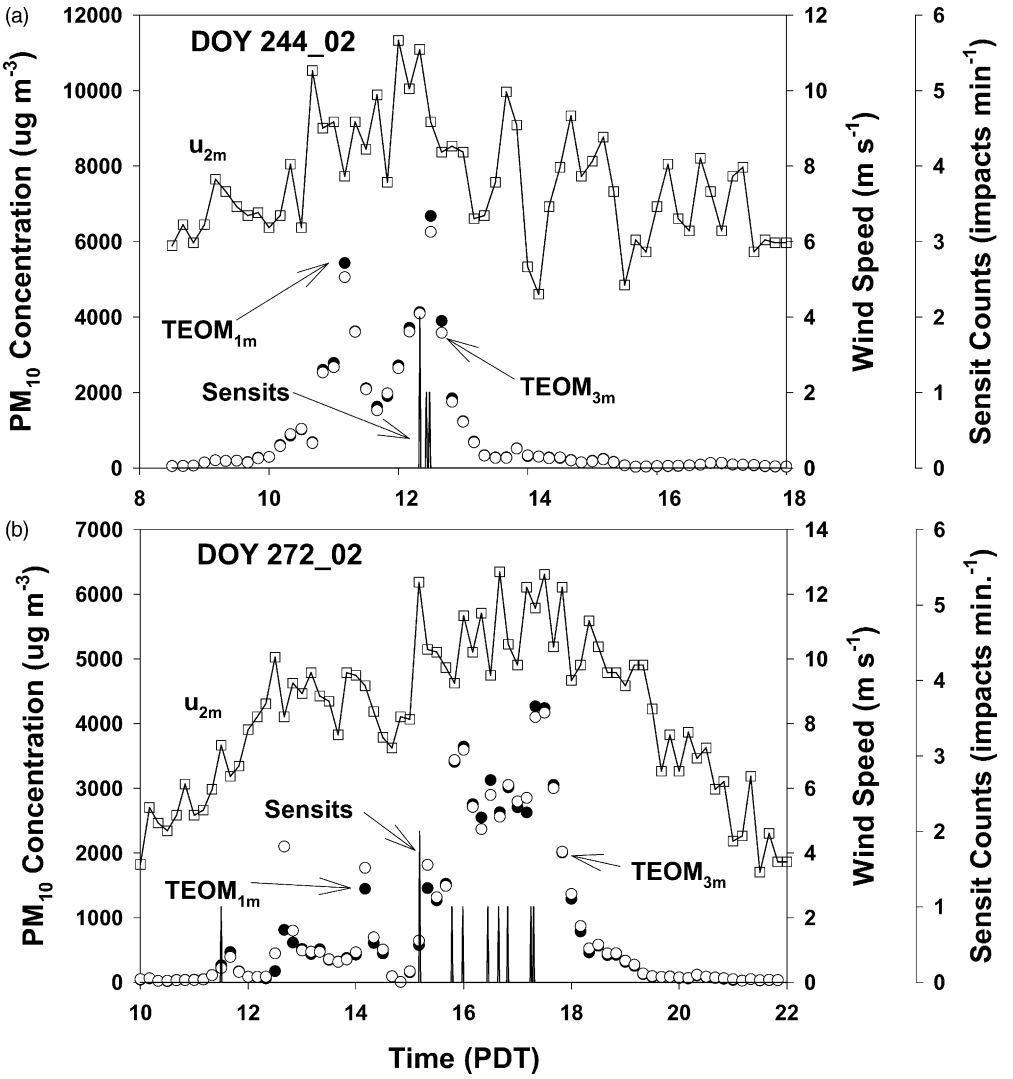

Fig. 5. The 10-min interval wind speed at 2 m (u_{2m}), TEOM PM_{10} concentrations at 1 and 3 m heights ($TEOM_{1m}$ and $TEOM_{3m}$) and particle impact counts per minute during high wind events on a) day-of year (DOY) 244, 2002; (b) DOY 272, 2002.

velocity measurements at all heights compared to the $TEOM_{3m}$ readings (Kjelgaard et al., 2004). Therefore, measurements of $TEOM_{1m}$ PM_{10} versus u_* for periods of increasing PM_{10} recorded during the four wind events are shown in Fig. 7. Except for a few isolated periods, apparent threshold u_* (u_{*t}) for rapid increases in PM_{10} emissions was approximately 0.4 m s^{-1}. By distinguishing periods of actively increasing PM_{10}, we reduced the influence of concentration lag periods when winds may decrease but PM_{10} concentrations will remain high because of the particles extremely low settling velocities ($\approx$0.008 m s^{-1}). However, considerable scatter in PM_{10} concentrations at higher u_* values were observed. The same PM_{10} readings were also compared to u_{2m} for the identical time periods. For DOY 285, DOY 244, and DOY 272 the vast majority of periods of elevated PM_{10} were during times when wind speed at 2 m height was greater than 8 m s^{-1}. However, this trend, also reflected in u_* values, did not hold for DOY 283 (discussed below).

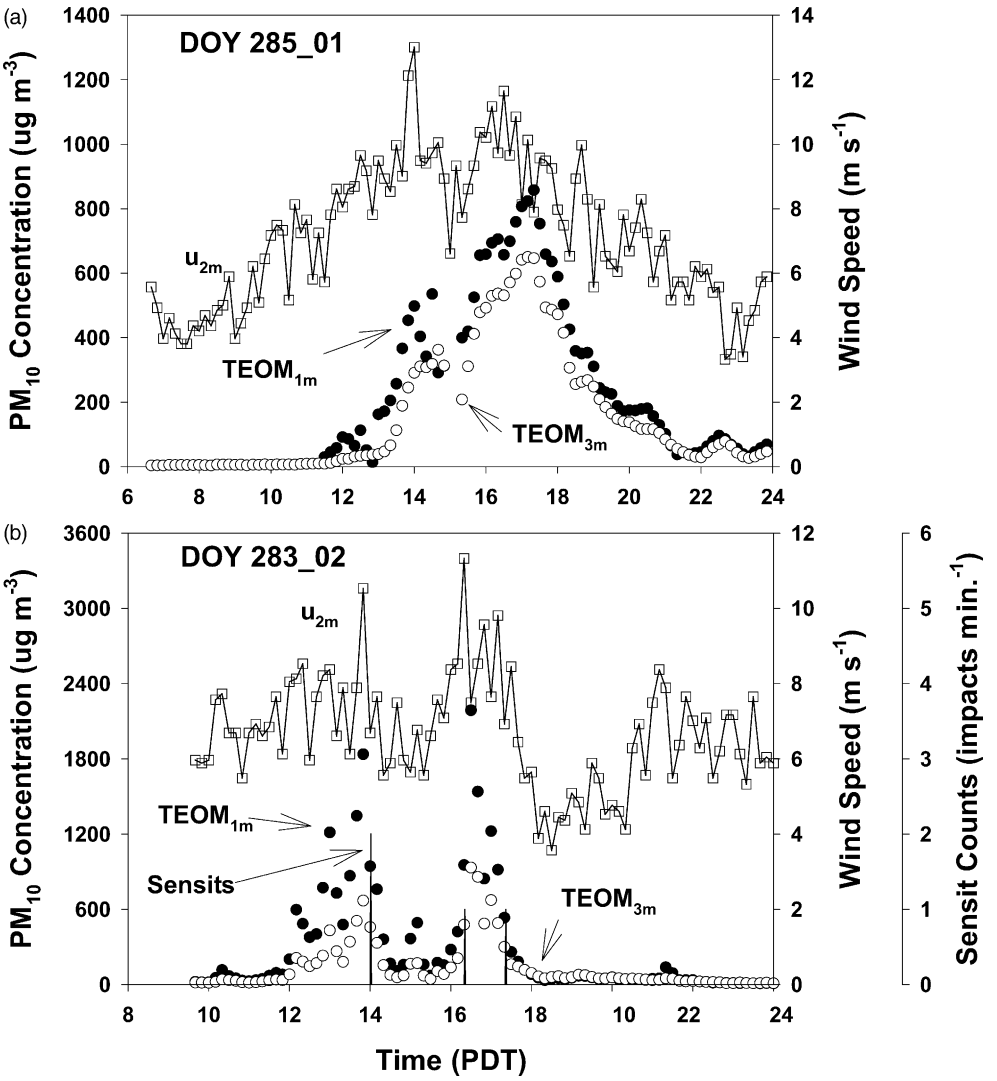

Fig. 6. The 10-min interval wind speed at 2 m (u_{2m}), TEOM PM_{10} concentrations at 1 and 3 m heights ($TEOM_{1m}$ and $TEOM_{3m}$) and particle impact counts per minute during high wind events on (a) day-of year (DOY) 285, 2001; (b) DOY 283, 2002.

Saltation can impact wind velocity profiles and is often referred to as the Owen effect (Owen, 1964; Gillette, 1999). This effect is due to the additional particle load on the lower part of the wind velocity profile, the shear stress being partitioned between the air and the particles carried in the airstream. In Owen's analysis, two key assumptions were that the saltating particles produced a momentum sink scaled to the particles maximum bounce height and that the air shear stress at the surface was just enough to keep saltating particles in motion. As more particles become entrained, the overall shear stress increases. Therefore, the Owen effect becomes more pronounced when the saltator's particle threshold velocity has been exceeded and depends on surface roughness conditions prior to saltation (Gillette et al., 1997). In field measurements, an increase in the ratio of u_* to mean wind speed is the easiest way to detect Owen effect (Gillette, 1999). We examined u_* and u_{2m} for DOY 272 and DOY 283 (Fig. 8a and b, respectively), representing the range

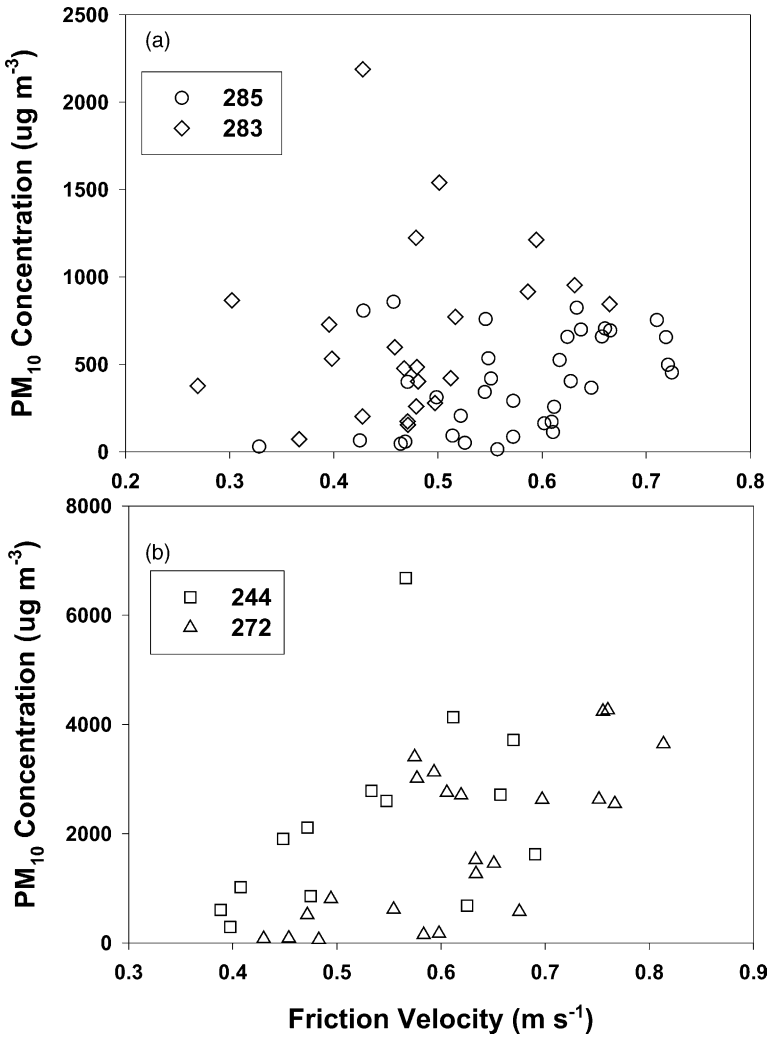

Fig. 7. The 10-min interval PM_{10} concentration at 1 m height (measured using TEOM) vs. wind profile friction velocity (u_*) during periods of increasing PM_{10} concentrations for high wind events on (a) day-of-year (DOY) 285, 2001 and DOY 283, 2002; (b) DOY 244, 2002 and DOY 272, 2002.

of dust storm intensities examined. In addition, atmospheric stability (as determined by *Ri*) was used to differentiate u_* values (Frank and Kocurek, 1994). The linearity of best-fit lines to both plots is apparent; DOY 283 had r^2 of 0.86 and DOY 272 had an r^2 of 0.93. The 95% confidence intervals demonstrate excellent fitting of the linear regressions. No stability effects on u_* values are noticeable and conditions were near-neutral during both events (*Ri* values were -0.004 ± 0.020 for DOY 272 and -0.004 ± 0.060 for DOY 283).

5. Discussion

The use of TEOMs can greatly enhance the quantity and quality of data on dust emissions from remote field sites. Previous studies in the Columbia Plateau region have only been able to utilize time integrated measurements with sampling times limited to periods of high winds. As seen in Fig. 2, high winds do not necessarily generate large amounts of dust. It is not uncommon for regional storms to have periodic high winds but only one large, main dust event associated with the passage

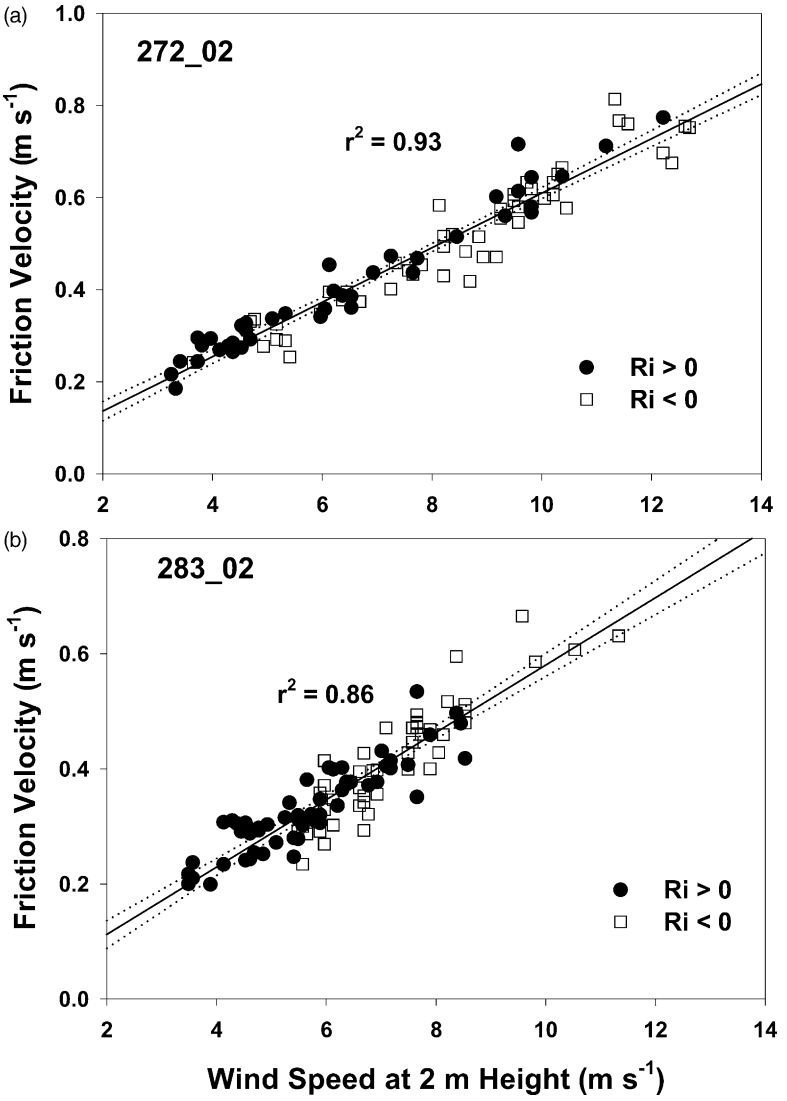

Fig. 8. The 10-min interval friction velocity (u_*) vs. wind velocity at 2 m (u_{2m}) during high wind events on (a) day-of-year (DOY) 272, 2002; (b) DOY 283, 2002. The u_* values are based on wind velocity measured between 0.1 and 5 m heights and differentiated by sign of Richardson's number (*Ri*).

of a frontal system. The PM_{10} concentrations obtained with TEOMs were extremely useful for targeting time periods of active emissions during a dust storm.

The overall performance of the TEOM was extremely good, and HWE time-integrated TEOM PM_{10} concentrations were in close agreement with PM_{10} concentrations measured using HiVols. Only one period (DOY 269–274) showed significant differences. On DOY 269, TEOMs at each height registered PM_{10} concentrations greater than 10,000 $\mu g\,m^{-3}$ for isolated periods while unloading equipment at the site. Both HiVol and TEOM filters were changed on DOY 269 during a period of little dust. Accordingly, TEOM readings from DOY 269 were discarded. In addition, the strongest HWE of the 2002 season occurred on DOY 272. Ono et al. (2000), while comparing 24-h

integrated PM_{10} concentrations, found TEOM measurements were consistently greater than those determined by HiVols. They sampled during calm periods and high intensity dust storms and attributed the differences to inlet efficiency changes under high winds and sample loss while handling heavily loaded HiVol filters. However, their range of PM_{10} measurements was relatively narrow, 0–200 $\mu g\,m^{-3}$, with a majority less than 100 $\mu g\,m^{-3}$. Noting the operational principle of the TEOM (Patashnick and Rupprecht, 1991), the effect of total particle load (μg) on the TEOM filter was also examined (Fig. 3a). By the end of period DOY 269–274, the TEOM filter weighed approximately 4500 μg. In comparison, the DOY 241–247 period, which had similar time-integrated PM_{10} concentrations, ended with a filter mass of approximately 2500 μg. The DOY 248–255 period had a relatively high TEOM filter mass, 3800 μg, but PM_{10} concentrations were relatively low. In both cases, the TEOM and HiVol results were very similar. Further examination of BSNE data showed that the DOY 269–274 period resulted in the greatest BSNE catch at each height, nearly twice the amounts trapped from periods with similar PM_{10} concentrations, DOY 241–247 and DOY 262–268. Therefore, the higher PM_{10} concentration indicated by the TEOM for DOY 269–274 was considered more accurate. Overall, the TEOMs appeared capable of supplying reliable reference readings of PM_{10} concentrations from soil-based emission sources.

Time-integrated streamwise soil mass transport is a complex phenomenon and beyond the scope of the current experiment to fully investigate. This study, however, does provide base-line information on emissions from a uniformly disturbed surface that is relatively dry, smooth, and devoid of plant residue. These field conditions are prevalent in the Fall when the strongest HWEs often occur on the Columbia Plateau. The simple and rugged design of BSNE samplers combined with their near-isokinetic sampling performance provided reliable estimates of horizontal soil flux. Stetler and Saxton (1996) found excellent correlation between horizontal soil flux and PM_{10} filter mass and vertical dust flux. Our results showed excellent agreement between horizontal soil flux and wind energy, W_e (Eq. (6) and Fig. 4a).

Time-integrated W_e and PM_{10} concentrations from 1, 3, and 5 m heights showed evidence of an extremely well-mixed PM_{10} profile for our field conditions (Fig. 4b). The non-linear response in PM_{10} concentrations to wind speed is also evident during individual storms (Fig. 5). The event-averaged mixing phenomenon appears to need a threshold W_e and to our knowledge has not been reported previously. Stetler and Saxton (1996) found that vertical dust flux decreased with increasing u_* and opined that this trend may have been due in part to a well-mixed dust concentration profile. Tsoar and Pye (1987) modeled PM_{10} concentrations with height for severe wind storm conditions ($u_* = 0.7\,m\,s^{-1}$) and found virtually no concentration gradient for heights from 1 m up to 100 m. With our fine loess soils and fallow conditions, there are limitations when using PM_{10} concentration measurements within certain height ranges for estimating PM_{10} vertical fluxes. In our study, integrated PM_{10} concentration gradients were evident between 1 and 5 m but with decreasing gradients for the stronger wind events (e.g. DOY 269–274, Fig. 4b). This suggests that PM_{10} flux gradient measurements determined with Eq. (1) require concentration measurements nearer to the eroding surface (<1 m height). Dynamic measurements of PM_{10} concentrations also illustrate the lack of concentration gradients during select wind events (Fig. 5). This provides some physical evidence that PM_{10} levels can attain well-mixed concentration profiles on the leeward side of large fields.

Estimates of PM_{10} fluxes were quite varied. For example, DOY 272 had negative fluxes occurring over the course of the HWE and the most negative 10-min flux, $-232\,ug\,m^{-2}\,s^{-1}$, nearly equaled the maximum positive 10-min flux estimated during our measurements, $258\,ug\,m^{-2}\,s^{-1}$ on DOY 283. Negative fluxes occurred predominantly after the strongest winds had passed. However, DOY 272 displayed averaged negative fluxes even for periods of increasing winds (i.e. Fig. 8). Unfortunately, no independent measurements of dust deposition were taken during this field campaign. However, both large regional HWEs, DOY 244 and 272, resulted in lower average PM_{10} fluxes than storms on DOY 283 and 285 despite the fact that DOY 244 and 272 experienced greater wind velocities and PM_{10} concentrations. We attributed this to upwind sources (i.e. several thousand hectares of fields with similar soils and surface conditions) and indicate that the effect of upwind sources may confound measurements if not accounted for. A similar pattern was seen for dust storms examined by Nickling et al.

(1999) over a 4-year period where regional storms also displayed lower vertical dust fluxes. The effect of negative fluxes and limited data set did confounded attempts to relate event-averaged dust flux magnitude to u_* (e.g. Gillette, 1977; Nickling, 1978; Nickling and Gillies, 1993; Nickling et al., 1999). Overall, the averaged fluxes are similar in magnitude to measurements done over agricultural lands (Gillette, 1977; Sabre et al., 1997).

Dynamic measurements of PM_{10} (Figs. 5 and 6) illustrate some very unique characteristics of the loess soils of the Columbia Plateau. Saltation appeared to be virtually non-existent (Figs. 5 and 6) as compared to other studies. For example, Gillette et al. (1997), Stout and Zobeck (1996, 1997), and Sterk and Spaan (1997) recorded saltation impact rates from tens to thousands of impacts per minute and on a near-continuous basis. This would imply several hundred to tens of thousands of saltating particles moving per minute per meter of field width. In contrast, our most intense storm, DOY 272, recorded 10 impacts total, distributed throughout the course of the HWE. A limited supply of saltator-sized particles (Lopez, 1998) could explain some of the data seen in Fig. 5 but was unlikely due to the large field size. The PSD distributions indicated 10–35% of particles were 90 μm in diameter or larger. In general, Ritzville soils are generally characterized by a relatively small mass percentage (15%) of aggregates with mean diameters between 90 and 180 μm; this diameter range encompasses the majority of saltators (Gillette and Chen, 1999). In addition, there were no flurries of saltation activity recorded during the early stages of the HWEs. Loosmore and Hunt (1998) reported that saltation could be suppressed in dry and loose sand/clay mixtures if the fraction of clay particles was large enough. A dry dust mulch condition could mimic this effect but still leaves the surface prone to dust emissions via direct suspension. Stout and Zobeck (1997) noted that smaller particles (<100 μm) need proportionally higher velocities to induce impact recordings with Sensits®. The Sensits® were tested in a wind tunnel (at wind velocities of $6\,m\,s^{-1}$) prior to field installation. However, at that time the soil was directly discharged into the tunnel air stream (i.e. not lifted off the tunnel floor). Scanning electron microscope (SEM) images of loose surface particles up to 125 μm mean diameter revealed flat, platy, and angular particle structures consistent with the glacial and volcanic sources of the loess material (Kjelgaard, unpublished data). Rice (1991), in wind tunnel studies, found that particles with reduced sphericity were more likely to be aerodynamically entrained, less likely to saltate, and if saltation occurred, less energetic in subsequent rebounds with the surface (i.e. reduced sand-blasting effect).

Threshold u_* velocities for PM_{10} emissions are illustrated in Fig. 7. Overall, the results seem very uniform except for DOY 283. However, the reduced threshold values on DOY 283 are easily explained by the positioning of perched particles (Bagnold, 1941) following the rod-weeding operations on DOY 281. This data illustrates the importance of accounting for timeliness when estimating PM_{10} emissions from agricultural production lands. The fields are most susceptible to PM_{10} emissions on days immediately following mechanized soil disturbances. It should also be noted that the values shown were for 10-min averages. Stetler and Saxton (1997) and Stout (1998) analyzed wind data and found that averaging times could greatly affect the magnitude of threshold velocities, a factor to be considered when comparing threshold velocity data.

The linearity of the plots of u_* versus u_{2m} (Fig. 8) for two storms, DOY 272 and DOY 283, show a relative constancy of the u_*/u ratio and give no indication of roughness height modification due to increases saltation. As mentioned, the stability conditions were neutral or near-neutral for all HWEs and no effects of stability on u_* calculations are apparent (Frank and Kocurek, 1994). The 95% confidence intervals indicate an excellent fit of the linear regression lines. Gillette et al. (1998) showed the Owen effect noticeably when u_t was exceeded by approximately 15% or more. Kjelgaard et al. (2004) calculated particle threshold velocities for 45 and 90 μm diameter particles (representing a mean surface and typical saltator-sized particles) and found no Owen effect for all wind speeds observed ($5–14\,m\,s^{-1}$) during two prior regional dust storms. For comparison, the event-integrated PM_{10} concentrations for those HWEs were approximately 1500 and $2500\,\mu g\,m^{-3}$, much greater than the range of concentrations seen in this study. This finding in addition to the extremely low number of saltation impacts recorded give further credence to the direct suspension mechanism for particle transport for soils on the Columbia Plateau.

6. Conclusions

A dryland agricultural field site on the Columbia Plateau in Washington State was monitored for soil erosion and PM_{10} emissions. The site was instrumented for measuring meteorological information, time-integrated soil erosion, time-integrated PM_{10} concentrations, and dynamic 10-min interval PM_{10} concentrations. Several dust events were monitored during 2001 and 2002.

Our data indicate the excellent agreement in PM_{10} concentrations as measured by tapered element oscillating microbalances and time-integrated HiVol samplers, during intermittent high wind conditions over periods of 5–10 days. The TEOM time-integrated performance exhibited sensitivity to filter mass loading. Time-integrated measurements of horizontal soil movement with BSNE samplers showed good correlation with PM_{10} concentrations collected over the same time periods. The time-integrated soil movement and PM_{10} concentrations showed correlation with wind energy (W_e) that utilized a threshold velocity of $8\,m\,s^{-1}$. Time-integrated concentration profiles of PM_{10} concentrations were well-mixed during large wind/dust events. PM_{10} concentrations were similar at heights of 1, 3 and 5 m for the strongest wind event of the season. Storms of lesser magnitude exhibited similar concentrations at 1 and 3 m heights while the weakest dust events showed substantial PM_{10} concentration differences between all heights. These observations show that careful consideration should be given when establishing measurement heights for determining gradient-based estimates of vertical dust flux (i.e. a flux-gradient method).

Saltation was not evident during high wind events. Saltator impact sensors recorded very few impacts during individual storms. An aerodynamic analysis based on wind velocity profile regression also showed no evidence of substantial saltation occurring and substantiates earlier work of Kjelgaard et al. (2004).

Periods of increasing PM_{10} emissions were examined during four events. The emission of PM_{10} from these soils appears to occur at a threshold u_* of $0.4\,m\,s^{-1}$ and an approximate threshold u_{2m} value of $8\,m\,s^{-1}$. However, soil disturbances can result in reduced threshold values, 0.3 and $6\,m\,s^{-1}$ for u_* and u_{2m}, respectively, due to perched particles. Event-averaged PM_{10} fluxes demonstrated smaller and even negative fluxes (deposition) for larger regional storms. All wind events showed some periods of negative fluxes for 10-min averaged fluxes after wind speeds had peaked. For dust flux experiments encompassing large field areas, independent measurements of dust deposition are recommended.

Acknowledgements

The authors would like to acknowledge the technical assistance of Robert Barry with various aspects of field and laboratory research. Dr. Alan Busacca's lab conducted the laser particle size analysis. The comments and questions from our reviewers were greatly appreciated. Funds for the research were provided by the USDA-ARS CP3 Project. Additional resources were provided by Washington State University. Products or manufacturers mentioned in the text are not endorsed by participating institutions or agencies.

References

Anderson, R.S., Haff, P.K., 1991. Wind modification and bed response during saltation of sand in air. Acta Mech. 1, 21–51.

Bagnold, R.A., 1941. The Physics of Blown Sand and Desert Dunes. Methuen, New York, pp. 265.

Brazel, A.J., 1989. Dust and climate in the American southwest. In: Leinen, M., Sarnthein, M. (Eds.), Paleoclimatology and Paleometeorology: Modern and Past Patterns of Global Atmospheric Transport. John Wiley & Sons Ltd., New York, pp. 65–96.

Butler, H.J., Hogarth, W.L., McTainsh, G.H., 2001. Effects of spatial variations in source areas upon dust concentration profiles during three wind erosion events in Australia. Earth Surf. Proc. Landforms 26, 1039–1048.

Cahill, T.A., Gill, T.E., Reid, J.S., Gearhart, E.A., Gillette, D.A., 1996. Saltating particles, playa crusts and dust aerosols at Owens (dry) lake, California. Earth Surf. Proc. Landforms 21, 621–639.

Campbell, C.D., 1962. Introduction to Washington Geology and Resources. Washington Department of Conservation, Olympia, W.A.

Chepil, W.S., Woodruff, N.P., 1957. Sedimentary characteristics of dust storms. Part I.I. Visibility and dust concentration. Am. J. Sci. 255, 104–114.

Chepil, W.S., Woodruff, N.P., 1963. The physics of wind erosion and its control. In: Norman, A. (Ed.), Advances in Agronomy. Academic Press, New York.

Claiborn, C., Lamb, B., Miller, A., Beseda, J., Clode, B., Vaughan, J., Kand, L., Newvine, C., 1998. Regional measurements and modeling of windblown agricultural dust: the Columbia Plateau PM_{10} program. J. Geophys. Res. 103, 19753–19767.

Donaldson, K., MacNee, W., 1998. The mechanism of lung injury caused by PM_{10}. In: Hester, R.E., Harrison, R.M. (Eds.), Issues in Environmental Science and Technology 10: Air Pollution and Health. The Royal Society of Chemistry, Cambridge, UK, pp. 21–32.

Frank, A., Kocurek, G., 1994. Effects of atmospheric conditions on wind profiles and Aeolian sand transport with an example from White Sands national monument. Earth Surf. Proc. Landforms 19, 735–745.

Fryear, D.W., 1984. Soil ridges-clods and wind erosion, Trans. ASAE, 445–448.

Fryear, D.W., 1986. A field dust sampler. J. Soil Water Cons. 41, 117–119.

Gillette, D., 1977. Fine particulate emissions due to wind erosion. Trans. ASAE 20, 890–897.

Gillette, D.A., 1986. Dust production by wind erosion: necessary conditions and estimates of vertical fluxes of dust and visibility reduction by dust. In: El-Baz, F., Hassan, M.H.A. (Eds.), Physics of Desertification. Martinus Nijhoff Publishers, Dordrecht, The Netherlands, pp. 361–371.

Gillette, D.A., 1999. Physics of Aeolian movement emphasizing changing of the aerodynamic roughness height by saltating grains (the Owen effect). In: Goudie, A.S., Livingstone, I., Stokes, S. (Eds.), Aeolian Environments, Sediments, and Landforms. John Wiley & Sons Ltd., New York, pp. 129–142.

Gillette, D.A., Chen, W., 1999. Size distributions of saltating grains: an important variable in the production of suspended particles. Earth Surf. Proc. Landforms 24, 449–462.

Gillette, D.A., Walker, T.R., 1977. Characteristics of airborne particles produced by wind erosion of sandy soil, high plains of west Texas. Soil Sci. 123, 97–110.

Gillette, D.A., Blifford, I.H., Fenster, C.R., 1972. Measurements of aerosol size distributions and vertical fluxes of aerosols on land subject to wind erosion. J. Appl. Meteorol. 11, 977–987.

Gillette, D.A., Blifford, I.H., Fryear, D.W., 1974. The influence of wind velocity of the size distributions of aerosols generated by the wind erosion of soils. J. Geophys. Res. 79, 4068–4075.

Gillette, D.A., Marticorena, B., Bergametti, G., 1998. Change in the aerodynamic roughness height by saltating grains: experimental assessment, test of theory, and operational parameterization. J. Geophy. Res. 103, 6203–6209.

Gillette, D.A., Fryear, D.W., Gill, T.E., Ley, T., Cahill, T.A., Gearhart, E.A., 1997. Relation of vertical flux of particles smaller than 10 μm to total aeolian horizontal mass flux at Owens Lake. J. Geophys. Res. 102, 26009–26015.

Ginoux, P., Chin, M., Tegen, I., Prospero, J.M., Holben, B., Dubovik, O., Lin, S.-J., 2001. Sources and distributions of dust aerosols simulated with the GOCART model. J. Geophys. Res. 106, 20255–20273.

Glenn, R.E., Craft, B.F., 1986. Air Sampling for Particulates. DHHS (NEDSH) Pub. No. 86–102. Occupational Respiratory Diseases. US Department of Health and Human Services, pp. 69–82.

Gomes, L., Arrue, J.L., Lopez, M.V., Sterk, G., Richard, D., Gracia, R., Sabre, M., Gaudichet, A., Frangi, J.P., 2003. Wind erosion in a semiarid agricultural area of Spain: the WELSONS project. Catena 745, 1–22.

Goosens, D., Gross, J., 2002. Similarities and dissimilarities between the dynamics of sand and dust during wind erosion of loamy sandy soil. Catena 47, 269–289.

Goosens, D., Gross, J., Spaan, W., 2001. Aeolian dust dynamics in agricultural land areas in lower Saxony, Germany. Earth Surf. Proc. Landforms 26, 701–720.

Hagen, L.J., Lyles, L., 1985. Amount and Nutrient Content of Particle Produced by Soil Aggregate Abrasion. Erosion and Soil Productivity. ASAE Pub. No. 8–85, pp. 117–129.

Hagen, L.J., Skidmore, E.L., 1976. Wind Erosion and Visibility Problems. Annual Meeting Technical Papers, No. 76–2019, American Society of Agricultural Engineers Annual Meeting, 27–30 June, Lincoln, N.E., 15 pp.

Horning, L.B., Stetler, L.D., Saxton, K.E., 1998. Surface residue and soil roughness for wind erosion protection. Trans. ASAE 41 (4), 1061–1065.

Houser, C.A., Nickling, W.G., 2001. The emission and vertical flux of particulate matter <10 μm from a disturbed clay-crusted surface. Sediment 48, 255–267.

Kjelgaard, J., Stockle, C.O., Evans, R.G., 1996. Accuracy of canopy temperature energy balance for determining daily evapotranspiration. Irrig. Sci. 16, 149–157.

Kjelgaard, J., Chandler, D., Saxton, K.E., 2004. Evidence for direct suspension of loessial soils on the Columbia Plateau. Earth Surface Process. Landforms 29, 221–236.

Larney, F.J., Bullock, M.S., Janzen, H.H., Ellert, B.H., Olson, E.C.S., 1998. Wind erosion effects on nutrient redistribution and soil productivity. J. Soil Water Conserv. 53, 133–140.

Ley, T.W., Muzzy, A.S., 1992. Experiences with an RF Telemetry-Based Automated Weather Station Network in Washington State. Annual Meeting Technical Papers, No. 922144, American Society of Agricultural Engineers Annual Meeting, 21–24 June, Charlotte, N.C., 21 pp.

Leys, J., 1999. Wind erosion on agricultural land. In: Goudie, A.S., Livingstone, I., Stokes, S. (Eds.), Aeolian Environments, Sediments, and Landforms. John Wiley & Sons Ltd., New York, pp. 143–166.

Leys, J.F., McTainsh, G.H., 1996. Sediment fluxes and particle grain-size characteristics of wind-eroded sediments in southeastern Australia. Earth Surf. Proc. Landforms 21, 661–671.

Leys, J., McTainsh, G.H., 1999. Dust and nutrient deposition to riverine environments of south-eastern Australia. Z. Geomorph. N.F. 116, 59–76.

Lodge, J.P., 1989. Methods of Air Sampling and Analysis. Lewis Publishers, New York, pp. 763.

Loosmore, G.A., Hunt, J.R., 1998. Predicting dust resuspension by considering saltator activity. In: Busacca, A. (Ed.), Dust Aerosols, Loess Soils and Global Change: An Interdisciplinary Conference and Field Tour on Dust in Ancient Environments and Contemporary Environmental Management. Seattle, W.A., USA, pp. 63–66.

Lopez, M.V., 1998. Wind erosion on agricultural soils: an example of limited supply of particles available for erosion. Catena 33, 17–28.

Lu, H., Shao, Y., 1999. A new model for dust emission by saltation bombardment. J. Geophys. Res. 104, 16827–16842.

Marks, H.M., 1996. Characteristics of Surface Soils that Affect Windblown Dust on the Columbia Plateau. Ph.D. Thesis. Washington State University, Pullman, W.A., USA.

Marticorena, B., Bergametti, G., 1995. Modeling the atmospheric dust cycle. Part 1. Design of a soil-derived dust emission scheme. J. Geophy. Res. 100, 16415–16430.

Nickling, W.G., 1978. Eolian sediment transport during dust storms: Slims River Valley, Yukon Territory. Can. J. Earth Sci. 15, 1069–1084.

Nickling, W.G., 1983. Grain-size characteristics of sediment transported during dust storms. J. Sediment. Petrol. 53 (3), 1011–1024.

Nickling, W.G., Gillies, J.A., 1993. Dust emission and transport in Mali, West Africa. Sediment 40, 859–868.

Nickling, W.G., McTainsh, G.H., Leys, J.F., 1999. Dust emissions from the Channel Country of western Queensland, Australia. Z. Geomorph. N.F. 116, 1–17.

Ono, D.M., Hardebeck, E., Parker, J., Cox, B.G., 2000. Systematic biases in measured PM_{10} values with US Environmental Protection Agency-approved samplers at Owens Lake, California. J. Air Waste Manage. Assoc. 50, 1144–1156.

Owen, P.R., 1964. Saltation of uniform grains in air. J. Fluid Mech. 20, 225–242.

Patashnick, H., Rupprecht, E.G., 1991. Continuous PM-10 measurements using the tapered element oscillating microbalance. J. Air Waste Manage. Assoc. 41, 1079–1083.

Pietersma, D., Stetler, L.D., Saxton, K.E., 1996. Design and aerodynamics of a portable wind tunnel for soil erosion and fugitive dust research. Trans. ASAE 39 (6), 2075–2083.

Pope, C.A., Dockery, D.W., 1999. Epidemiology of particle effects. In: Holgate, S.T., Samet, J.M., Koren, H.S., Maynard, R.L. (Eds.), Air Pollution and Health. Academic Press, New York, pp. 673–705.

Pye, K., 1987. Aeolian Dust and Dust Deposits. Academic Press, New York, pp. 334

Raupach, M.R., 1991. Saltation layers, vegetation canopies and roughness lengths. Acta Mech. 1, 83–96.

Raupach, M.R., Leys, J.F., 1990. Aerodynamics of a portable wind erosion tunnel for measuring soil erodibility by wind. Aust. J. Soil Res. 28, 177–191.

Rice, M.A., 1991. Grain shape effects on aeolian sediment transport. Acta Mech. 1, 159–166.

Sabre, M., Lopez, M.V., Alfaro, S.C., Rajot, J.L., Gomes, L., 1997. Characterization of the fine dust particle production process by wind erosion for two types of bare soil surfaces. In: Proceedings of the Wind Erosion: an International Symposium/Workshop, 3–5 June 1997. Manhattan, Kansas: USDA-ARS.

Saxton, K.E., 1995. Wind erosion and its impact on off-site air quality in the Columbia Plateau—an integrated research plan. Trans. ASAE 38 (4), 1031–1038.

Saxton, K.E., Chandler, D., Stetler, L., Lamb, B., Claiborn, C., Lee, B.H., 2000. Wind erosion and fugitive dust fluxes on agricultural lands in the Pacific Northwest. Trans. ASAE 43 (3), 623–630.

Shao, Y., 2000. Physics and Modelling of Wind Erosion. Kluwer Academic Publishers. Boston, Massachusetts, pp. 393.

Shao, Y., Raupach, M.R., Findlater, P.A., 1993. Effect of saltation bombardment on the entrainment of dust by wind. J. Geophy. Res. 98, 12719–12726.

Shao, Y., Raupach, M.R., Leys, J.F., 1996. A model for predicting Aeolian sand drift and dust entrainment on scales from paddock to region. Aust. J. Soil Res. 34, 309–342.

Sokolik, I., Toon, O., 1996. Direct radiative forcing by anthropogenic airborne mineral dust. Nature 318 (6584), 681–684.

Soutar, A., Watt, M., Cherrie, J.W., Seaton, A., 1999. Comparison between a personal PM_{10} sampling head and the tapered element oscillating microbalance (TEOM) system. Atmos. Environ. 33, 4373–4377.

Sterk, G., Spaan, W.P., 1997. Wind, erosion control with crop residues in the Sahel. Soil Sci. Soc. Am. J. 61, 911–917.

Stetler, L.D., Saxton, K.E., 1996. Wind erosion and PM_{10} emissions from agricultural fields on the Columbia Plateau. Earth Surf. Proc. Landforms 21, 673–685.

Stetler, L.D., Saxton, K.E., 1997. Analysis of wind data used for predicting soil erosion. In: Proceedings of the Wind Erosion: an International Symposium/Workshop, 3–5 June 1997. Manhattan, Kansas: USDA-ARS.

Stout, J.E., 1998. Effect of averaging time on the apparent threshold for Aeolian transport. J. Arid Environ. 39, 395–401.

Stout, J.E., 2001. Dust and environment in the southern high plains of North America. J. Arid Environ. 47, 425–441.

Stout, J.E., Lee, J.A., 2003. Indirect evidence of wind erosion trends on the southern high plains of North America. J. Arid Environ. 55 (1), 43–61.

Stout, J.E., Zobeck, T.M., 1996. The Wolfforth field experiment: a wind erosion study. Soil Sci. 161, 616–632.

Stout, J.E., Zobeck, T.M., 1997. Intermitt. Saltat. Sediment. 44, 959–970.

Stull, R., 2000. Meteorology for Scientists and Engineers, second ed. Brooks/Cole. Pacific Grove, California, pp. 502.

Sutton, O.G., 1953. Micrometeorology a Study of Physical Processes in the Lowest Layers of the Earth's Atmosphere. McGraw-Hill, New York, pp. 333.

Tegen, I., Fung, I., 1995. Contribution to the atmospheric mineral aerosol load from land surface modification. J. Geophys. Res. 100, 18707–18726.

Thom, A.S., 1975. Momentum, mass and heat exchange of plant communities. In: Monteith, J.L. (Ed.), Vegetation and the Atmosphere, Academic Press, New York, pp. 57–109.

Tsoar, H., Pye, K., 1987. Dust transport and the question of desert loess formation. Sediment 34, 139–153.

U.S.D.A., 1967. Soil Survey: Adams County, Washington, p. 102.

Xuan, J., Sokolik, I.N., 2002. Characterization of sources and emission rates of mineral dust in northern China. Atmos. Environ. 36, 4863–4876.

Zingg, A.W., 1951. A portable wind tunnel and dust collector developed to evaluate the erodibility of field surfaces. Agron. J. 43, 189–191.

Zobeck, T.M., Fryear, D.W., 1986. Chemical and physical characteristics of windblown sediment. Part I. Quantities and physical characteristics. Trans. ASAE 29 (4), 1032–1036.